Level structure of ^{94,95,96}Tc at high spins and shell-model calculations

S. S. Ghugre,* B. Kharraja,† and U. Garg
Department of Physics, University of Notre Dame, Notre Dame, Indiana 46556

R. V. F. Janssens, M. P. Carpenter, B. Crowell,‡ T. L. Khoo, T. Lauritsen, and D. Nisius§
Physics Division, Argonne National Laboratory, Argonne, Illinois 60439

W. Reviol, W. F. Mueller,‖ and L. L. Riedinger
Department of Physics, University of Tennessee, Knoxville, Tennessee 37996

R. Kaczarowski
Soltan Institute for Nuclear Studies, 05-400 Swierk, Poland
(Received 16 September 1999; published 22 December 1999)

High-spin states in the ^{94,95,96}Tc ($N=51$, 52, and 53) nuclei have been investigated using the ^{65}Cu+^{36}S reaction at a beam energy of 142 MeV. More than 60 new transitions have been identified and placed in their level schemes, which now extend up to spin $J\approx 22\hbar$ and excitation energies $E_x\approx 12$ MeV. Spherical shell-model calculations have been performed using different model spaces. A restricted model space, using ^{88}Sr as the core and the $\pi(p_{1/2},g_{9/2})$ $\nu(d_{5/2},s_{1/2})$ valence orbitals, reproduces the experimental excitation energies up to $J\approx 14\hbar$. The higher-angular-momentum states are dominated by the excitation of a $g_{9/2}$ neutron across the $N=50$ magic core, as indicated by large-basis shell model calculations.

PACS number(s): 27.60.+j, 23.20.Lv, 21.60.Cs

I. INTRODUCTION

It is well established by now, both from experimental data and from spherical shell-model calculations, that in the $Z\sim 42-44$ region single-particle excitations dominate the level structures of nuclei with $N\leqslant 51$ even at rather high-angular momenta ($J\approx 20\hbar$, $E_x\approx 10$ MeV) [1,2]. On the other hand, nuclei with $N\geqslant 55$ exhibit collective behavior [3]. Until recently, very little was known about the $N=52-54$ intermediate nuclei. In order to understand these ''transitional nuclei,'' a program of extensive investigations of nuclei with $52\leqslant N\leqslant 54$ has recently been undertaken [4–6]. The study of the level structure of ^{94,95}Mo [5], $^{96-98}$Ru [4], and ^{97,98}Rh [6] has led to a detailed understanding of the mechanism responsible for the generation of high-spin states in this region. In these studies, extensive level schemes have been established up to rather high spins and excitation energies ($J\approx 22\hbar$, $E_x\approx 12$ MeV). Also, shell model calculations with a small configuration space (using ^{88}Sr as the core) were found to be in good agreement with the data for levels up to $J\approx 16\hbar$ (the maximum angular momentum possible within this restricted space). The use of larger configuration spaces has indicated that the higher-angular-momentum states are dominated by the excitation of a $\nu(g_{9/2})$ neutron across the $N=50$ shell gap. In particular, the observation of γ rays with $E_\gamma\approx 2$ MeV, and the associated fragmentation of the γ-ray flux, provided a clear experimental signature for the breaking of the $N=50$ core. Finally, in many of these nuclei, negative-parity sequences were found involving series of $E2$ transitions of which the energies increase with increasing spin. These ''rotational bandlike'' $E2$ cascades, although indicative of a possible onset of collectivity, were reproduced by shell model calculations.

In this paper, we report on our investigation of the high-spin states in the ^{94,95,96}Tc ($N=51$, 52, 53) nuclei. These nuclei were obtained as by-products in the study of $^{96-98}$Ru nuclei reported in Ref. [4].

II. EXPERIMENTAL METHODS

High-spin states in ^{94,95,96}Tc have been investigated using the early implementation phase of the Gammasphere spectrometer [7] which at the time comprised 36 large ($\geqslant 70\%$ relative efficiency) Compton Suppressed Germanium (CSGe) detectors. The ^{65}Cu+^{36}S reaction was used at a bombarding energy of 142 MeV. The ^{36}S beam was provided by the 88-in. Cyclotron facility at the Ernest O. Lawrence Berkeley National Laboratory. Two stacked, self-supporting, isotopically enriched ^{65}Cu target foils (~ 0.5 mg/cm^2 thick) were used. A total of about 4×10^8 events were accumulated and stored onto magnetic tapes for further analysis. Even though the chosen reaction conditions were not very conducive to the reaction channels leading to the $^{94-96}$Tc final nuclei, it was still possible to obtain substantial new information on the higher-angular-momentum states in these nuclei, as can be seen below. The most

*Present address: IUCDAEF-Calcutta Centre, Sector III/LB-8, Bidhan Nagar, Calcutta 700 091, India.

†On leave from Department of Physics, Université Chouaib Doukkali, BP20, El Jadida, Morocco.

‡Present address: Fullerton Community College, Fullerton, CA 92833.

§Present address: Bio-Imaging Research Inc., Lincolnshire, IL 60069.

‖Present address: NSCL, Michigan State University, East Lansing, MI 48824.

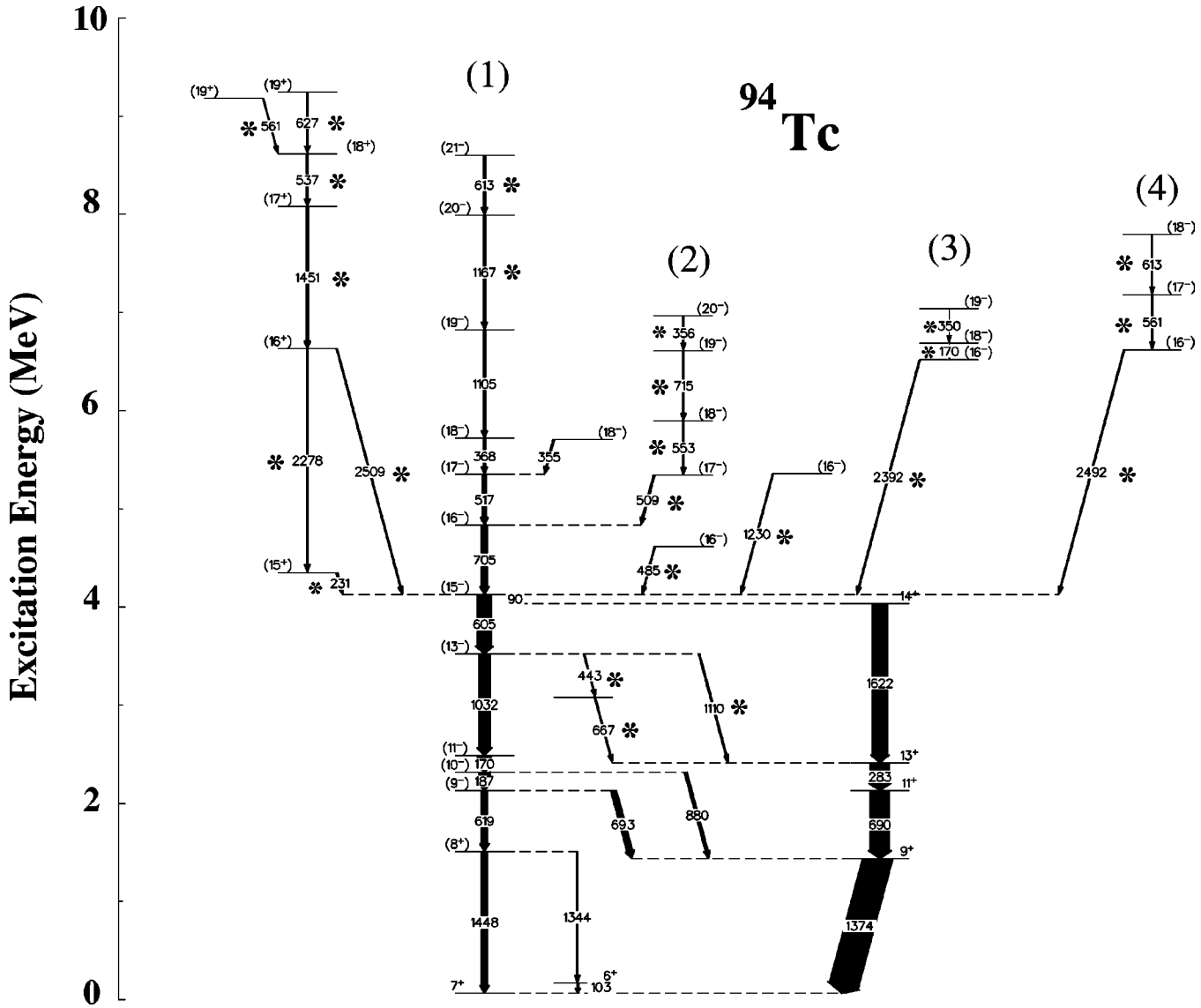

FIG. 1. Level scheme for ^{94}Tc as established from the present study. The transition energies are labeled in keV. The new transitions are indicated by an asterisk. The widths of the arrows are approximately equal to the relative intensities of the observed γ transitions.

strongly populated nuclei were the $^{96-98}$Ru isotopes, which were reported previously by Kharraja *et al.* [4]; the total γ-ray flux corresponding to the ^{94}Tc, ^{95}Tc, and ^{96}Tc nuclei in our data set was about 8, 12, and 4 % of the total reaction-yield, respectively.

The data were sorted into three-dimensional histograms ($E_\gamma - E_\gamma - E_\gamma$ cubes) using the Radware [8] and Kuehner [9] formats. The experimental details, including procedures for constructing level schemes, and for multipolarity assignments, are given in Ref. [4]. In particular, multipolarity assignments were based primarily on intensity ratios R, defined as $R = I_\gamma(\text{backward})/I_\gamma(90°)$, and extracted from angle-sorted matrices: coincidence gates were placed on transitions detected in the forward-angle (32° and 37° with respect to incoming beam direction) detectors, and the γ rays measured at 90° and at backward angles (143° and 147°) were sorted along the two axes of the matrices. Under these conditions, $E2$ transitions, typically, have R values of ~ 2 and $M1$'s ~ 1.5 (see, for example, Ref. [4]). Supporting evidence for the spin assignments is provided by crossover transitions observed in these nuclei.

III. RESULTS

A. Levels in ^{94}Tc

The level scheme of ^{94}Tc, as deduced from this work, is shown in Fig. 1 and a typical double-gated γ-ray coincidence spectrum is shown in Fig. 2. Prior to this work, the level structure of ^{94}Tc was known up to a spin of $J = 20\hbar$ and an excitation energy of $E_x \approx 7$ MeV [1]. A total of 25 new transitions has been placed in the level scheme of ^{94}Tc which has now been extended up to $E_x \approx 10$ MeV. The states below $J = 15\hbar$ are in agreement with the previous work [1]. The previously-known negative-parity sequence (sequence 1) included five transitions decaying from the 20^- level to the 15^- level [1]. The ordering of the γ-ray transitions of 705, 517, and 368 keV (366 keV in Ref. [1]) in this sequence has been changed, based on the observed intensity pattern and

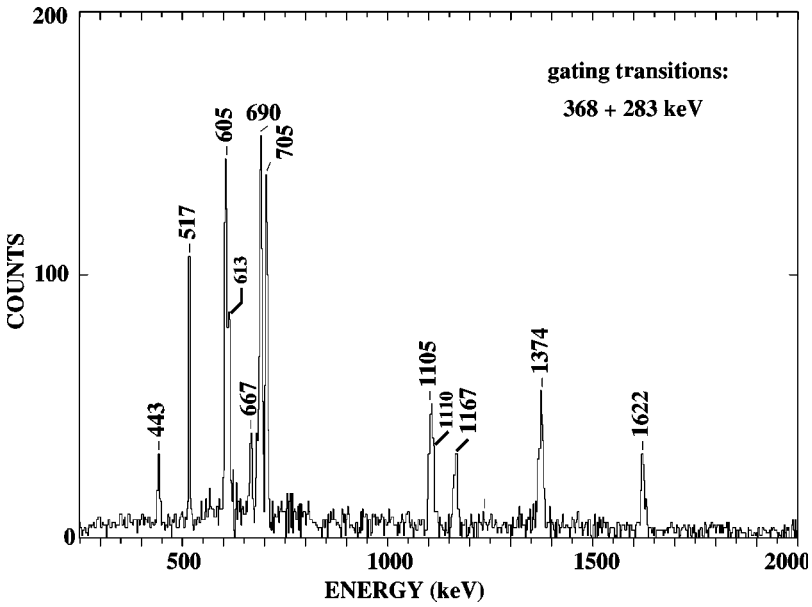

FIG. 2. Representative double-gated coincidence γ spectrum for ^{94}Tc. All transition energies are marked to within ± 1 keV. The spectrum has not been corrected for the efficiencies of the Ge detectors.

the coincidence relationships. Notice also that the 355-keV γ ray is not in coincidence with the four highest transitions of this sequence and, therefore, has been placed in parallel with the 368-keV transition. Three new crossover transitions have been observed at low spins between the positive- and negative-parity cascades; the energies of the corresponding γ rays are 443, 667, and 1110 keV, respectively. The major change in the level scheme compared to Ref. [1] is the observation of three new cascades with negative parity and one with positive-parity above spin 15 $\hbar$. The negative-parity cascades are labeled sequences 2, 3, and 4 in Fig. 1. The new transitions in these sequences are of energies of 509, 553, 715, and 356 keV for sequence 2; 2392, 170, and 350 keV for sequence 3; and, 2492, 561, and 613 keV for sequence 4. The positive-parity sequence consists of the following transitions: 231, 2278, 2509, 1451, 537, 627, and 561 keV. Several γ transitions with energies around 2 MeV (2278, 2509, 2392, and 2492 keV) feeding the (15^-) level have also been observed in the present work. The presence of these high-energy γ rays, and the associated fragmentation of the γ-ray flux into many competing pathways, is by now a well established feature for all $N=50-54$ nuclei and provides a clear experimental signature for the breaking of the $N=50$ core (see, for example, Ref. [4]). The measured spectroscopic data (γ-ray energies, intensities, intensity ratios R, and suggested spin assignments) are summarized in Table I.

B. Levels in ^{95}Tc

Figure 3 illustrates a typical double-gated coincidence spectrum for ^{95}Tc and the level scheme obtained for this nucleus is displayed in Fig. 4. 33 new transitions have been observed and unambiguously placed in the level scheme, which has been extended up to $J \geqslant 47/2\hbar$ and $E_x \approx 15$ MeV. In general, there is a good agreement with the results obtained previously [10] although some discrepancies need to be noted. The major change in the level scheme with respect to Ref. [10] is the nonobservation of the 608 and 1238 keV transitions feeding the $1/2^-$ ground state, and the absence of the 291-, 301-, 337-, 627-, 749-, 1179-, and 1265-keV transitions. These γ rays were associated with low-spin states in the positive-parity cascade in measurements using the ^{93}Nb(α, $2n\gamma$) reaction [10]. It is very likely that the states associated with these γ rays were not populated in the present work due to the use of the ^{36}S heavy-ion induced reaction which enhances population of yrast states with rather high spins.

The nucleus ^{95}Tc has also been investigated by other groups using the same ^{93}Nb(α, $2n\gamma$) reaction [11–14], and the ^{95}Mo(p, $n\gamma$)^{95}Tc reaction [15]. However, the information obtained from these studies has been limited primarily to low spins.

The new transitions belonging to the main negative-parity cascade (cascade 1) and feeding the $9/2^-$ level are of energies 487, 511, 812, 798, 1149, 860, 2467 keV, respectively. This cascade splits at the $(33/2^-)$ level into 5 pathways. The longest emerging cascade includes the 2089, 619, 720, 1400, 1419, and 2382 keV transitions and reaches $E_x \approx 15$ MeV. This group is labeled sequence 2 in Fig. 4. A third lateral sequence starts at the $(25/2^-)$ level and includes the 307-, 657-, 583-, 1134-, and 860-keV γ rays.

The positive-parity cascade terminates at lower spin and excitation energy when compared with the negative-parity cascade. The topmost transition in this cascade has an energy of 1000 keV and de-excites a level with $J^\pi=(37/2^+)$ and $E_x \approx 9$ MeV. The new transitions in this cascade have energies of 176, 177, 192, 403, 714, 970, 1000, 1069, 1681, and 1811 keV, respectively. Table II lists all the γ rays assigned to ^{95}Tc, along with their intensities, the intensity ratios R (where available), and the suggested placements in the level scheme.

C. Levels in ^{96}Tc

Although ^{96}Tc was one of the very weakly populated nuclei in this experiment, it was still possible to obtain valuable information on the level structure of this $N=53$ isotope.

TABLE I. Energies, initial and final spins, relative intensities, and the intensity ratios R (as defined in the text) for transitions assigned to ^{94}Tc.

E_γ(keV)[a]	$J_i \rightarrow J_f$[b]	I_γ[c]	R[d]
91.8	$(15^-)\rightarrow(14^+)$	7.7 (20)	1.3 (2)
103.4	$6^+\rightarrow 7^+$	6.0 (10)	1.6 (3)
170.0	$(11^-)\rightarrow(10^-)$	45	1.5 (3)
170.2	$(18^-)\rightarrow(16^-)$	4.0 (8)	
187.0	$(10^-)\rightarrow(9^-)$	32	1.6 (2)
231.3	$(15^+)\rightarrow(15^-)$	6.0 (10)	
283.4	$13^+\rightarrow 11^+$	65	1.9 (2)
350.1	$(19^-)\rightarrow(18^-)$	3.9 (6)	
355.2	$(18^-)\rightarrow(17^-)$	5.9 (10)	
356.2	$(20^-)\rightarrow(19^-)$	4.1 (6)	
368.1	$(18^-)\rightarrow(17^-)$	8.1 (11)	1.5 (2)
443.0		4.0 (7)	
485.1	$(16^-)\rightarrow(15^-)$	4.2 (7)	
509.0	$(17^-)\rightarrow(16^-)$	6.1 (9)	
517.1	$(17^-)\rightarrow(16^-)$	14	1.5 (3)
537.0	$(18^+)\rightarrow(17^+)$	7.9 (11)	1.6 (2)
553.1	$(18^-)\rightarrow(17^-)$	5.1 (9)	
561.0	$(17^-)\rightarrow(16^-)$	4.0 (7)	
561.1	$(19^+)\rightarrow(18^+)$	3.0 (5)	
605.2	$(15^-)\rightarrow(13^-)$	48	1.8 (2)
613.1	$(18^-)\rightarrow(17^-)$	3.0 (6)	
613.2	$(21^-)\rightarrow(20^-)$	8.1 (12)	1.6 (2)
619.2	$(9^-)\rightarrow(8^+)$	21	1.3 (2)
627.2	$(19^+)\rightarrow(18^+)$	4.9 (8)	
667.0		4.0 (8)	
690.4	$11^+\rightarrow 9^+$	67	1.9 (3)
693.0	$(9^-)\rightarrow(9^+)$	12	1.8 (2)
705.2	$(16^-)\rightarrow(15^-)$	20	1.5 (1)
715.2	$(19^-)\rightarrow(18^-)$	5.1 (13)	1.5 (2)
880.0	$(10^-)\rightarrow 9^+$	13	1.3 (2)
1032.0	$(13^-)\rightarrow(11^-)$	40	1.9 (2)
1105.2	$(19^-)\rightarrow(18^-)$	8.0 (9)	1.6 (2)
1110.0	$(13^-)\rightarrow 13^+$	5.2 (8)	
1167.1	$(20^-)\rightarrow(19^-)$	8.0 (11)	1.6 (2)
1230.1	$(16^-)\rightarrow(15^-)$	4.1 (7)	
1344.4	$(8^+)\rightarrow 6^+$	6.2 (12)	1.9 (2)
1374.0	$9^+\rightarrow 7^+$	100	2.0 (2)
1447.8	$(8^+)\rightarrow 7^+$	14	1.5 (2)
1451.1	$(17^+)\rightarrow(16^+)$	10	1.5 (2)
1622	$14^+\rightarrow 13^+$	50	1.5 (2)
2278	$(16^+)\rightarrow(15^+)$	6.1 (10)	
2392	$(16^-)\rightarrow(15^-)$	4.2 (9)	
2492	$(16^-)\rightarrow(15^-)$	4.1 (8)	
2509	$(16^+)\rightarrow(15^-)$	4.0 (10)	

[a]The transitions of energies $\leqslant$1500 keV are known to $\sim$0.4 keV; for the higher energies, the uncertainties are $\sim$1 keV.

[b]A blank space is kept for all the transitions for which the spins are not determined.

[c]Except where stated, the uncertainties in relative intensities are less than 10%.

[d]A blank space is kept for all the transitions for which R could not be obtained.

While only a limited number of transitions were placed in the level scheme, it was still extended up to spins and excitation energies comparable to those achieved in ^{94}Tc and ^{95}Tc. In effect, the level scheme was extended only *vertically* (i.e., along the ground-state ''band'') because of the rather limited data set.

^{96}Tc has also been studied in the past via the ^{93}Nb(α, $n\gamma$) fusion-evaporation reaction [16]. Many transitions were observed and placed in the level scheme at low spins: the highest spin and excitation energy reached in the previous measurements were only $J\approx 13\hbar$ and $E_x\approx 2.6$ MeV. Of all the γ rays reported in Ref. [16], only the 927-keV transition, feeding the ground state, is observed in the present study.

Due to the excellent efficiency for high-fold coincidence events provided by Gammasphere, we were able to observe and place 21 new γ transitions in the main positive parity cascade of the ^{96}Tc level scheme, extending it up to spin J $\approx 24\hbar$ and excitation energy $E_x\approx 11$ MeV. The level scheme of ^{96}Tc, as deduced from this work, is shown in Fig. 5 and a representative double-gated γ-ray coincidence spectrum is shown in Fig. 6. Table III summarizes the γ-ray energies, intensities, and intensity ratios R of all the observed transitions of ^{96}Tc.

IV. DISCUSSION

Spherical shell model calculations have been performed in order to explain the low-lying levels in the $N=51-54$ Mo, Tc, Ru, and Rh nuclei. For instance, the basis set with ^{88}Sr as the inert core and $[\pi(p_{1/2},g_{9/2});\nu(d_{5/1},s_{1/2})]$ valence orbitals (codenamed GL in the OXBASH code [17]) leads to reasonably good agreement between the experimental and calculated quantum numbers (spins, parities, and excitation energies) up to the maximum angular momentum possible for these nuclei using this small configuration space [4–6].

In particular, in an earlier work [1] the experimental values obtained in ^{94}Tc were reproduced rather well up to spin 15^- and 11^+ using this model space. As can be seen in Fig. 7, similar results are obtained in the present study as well. Also, the experimental excitation energy for the 14^+ level is about 2 MeV lower than in the shell-model predictions. This could be due to the omission of higher lying orbitals such as $g_{7/2}$ and $h_{11/2}$. Hence, to obtain a more appropriate description of this level and the higher spin states, large-basis shell model calculations are necessary. These calculations have been performed for ^{94}Tc using the model space named SNE in OXBASH, wherein the ^{56}Ni nucleus is used as the core. However, due to the large dimensionality of the m subspace resulting from the involvement of high-j orbitals such as $h_{11/2}$, a truncation scheme was employed, the details of which are provided in Ref. [2]. Figure 7 shows the comparison between the experimental excitation energies and the extended-basis shell model calculations. As can be seen, the agreement between the experimental and theoretical excitation energies now becomes quite satisfactory up to the highest observed states. Notice, however, that the experimental and the calculated excitation energies are still different for the level 16^+. A similar discrepancy has been observed in the Ru [4], Mo [5], and the Rh [6] nuclei and is likely related

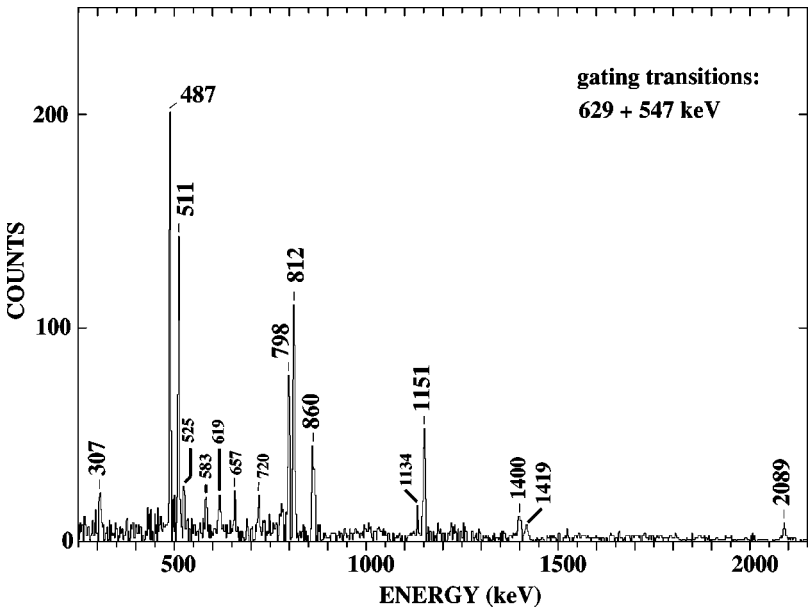

FIG. 3. Representative double-gated coincidence γ spectrum for the main positive-parity sequence of ^{95}Tc.

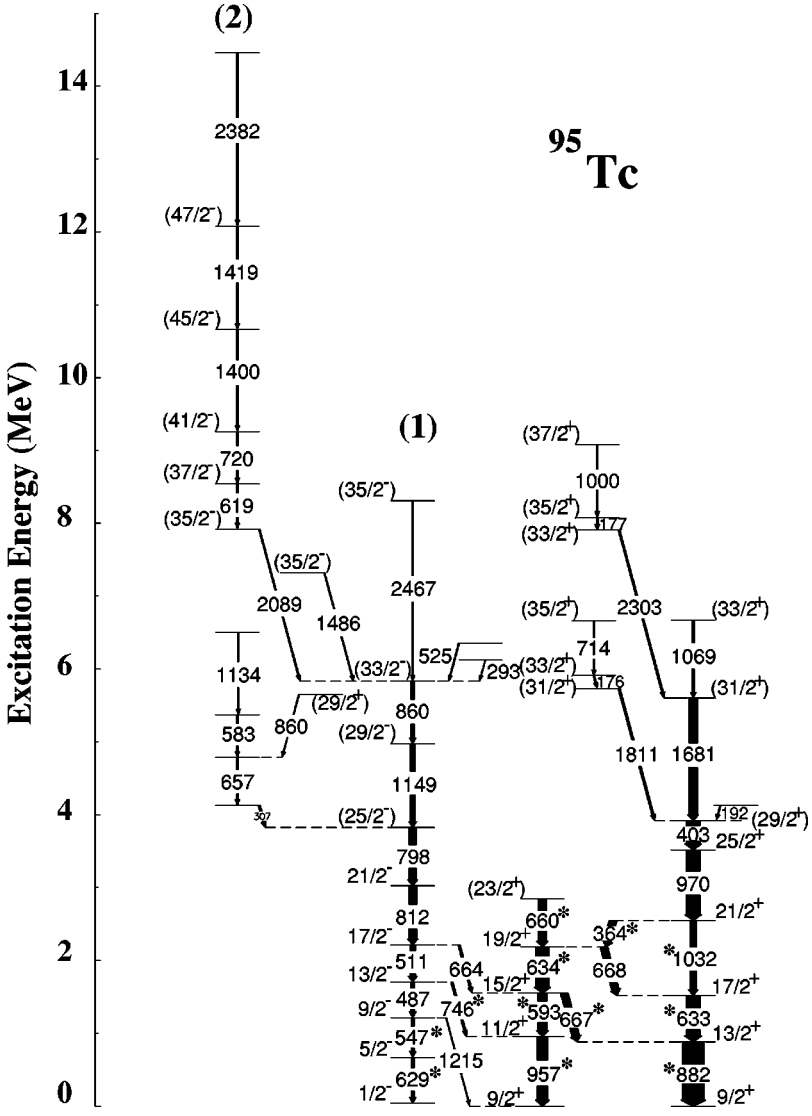

FIG. 4. Level scheme for ^{95}Tc as established from the present study. The previously known transitions are indicated by an asterisk.

TABLE II. Energies, initial and final spins, relative intensities, and the intensity ratios R (as defined in the text) for transitions assigned to ^{95}Tc.

E_γ(keV)[a]	$J_i \rightarrow J_f$[b]	I_γ[c]	R[d]	E_γ(keV)[a]	$J_i \rightarrow J_f$[b]	I_γ[c]	R[d]
176.1	$(33/2^+) \rightarrow (31/2^+)$	6.9 (9)		745.5	$13/2^- \rightarrow 11/2^+$	10	1.3(2)
177.2	$(35/2^+) \rightarrow (33/2^+)$	8.1 (10)		798.1	$(25/2^-) \rightarrow 21/2^-$	33	1.8(2)
192.1		5.2 (8)		812.0	$21/2^- \rightarrow 17/2^-$	36	2.0(3)
293.0		3.1 (6)		860.2	$(33/2^-) \rightarrow (29/2^-)$	16	2.1(2)
307.0	$(29/2^-) \rightarrow (25/2^-)$	10	2.1 (3)	860.1		4.2 (8)	
364.0	$21/2^+ \rightarrow 19/2^+$	35	1.5 (2)	882.3	$13/2^+ \rightarrow 9/2^+$	100	2.0(2)
403.1	$(29/2^+) \rightarrow 25/2^+$	63	1.9 (3)	956.6	$11/2^+ \rightarrow 9/2^+$	49	1.5(2)
487.0	$13/2^- \rightarrow 9/2^-$	18	1.9 (3)	970.1	$25/2^+ \rightarrow 21/2^+$	63	2.0(3)
511.0	$17/2^- \rightarrow 13/2^-$	26	2.0 (2)	1000.1	$(37/2^+) \rightarrow (35/2^+)$	6.1 (11)	
525.1		5.0 (10)		1032.0	$21/2^+ \rightarrow 17/2^+$	30	1.9(3)
547.0	$9/2^- \rightarrow 5/2^-$	15	2.1 (3)	1069.2	$(33/2^+) \rightarrow (31/2^+)$	12	1.6(2)
583.1		6.0 (9)		1134.2		3.1 (11)	
593.0	$15/2^+ \rightarrow 11/2^+$	42	1.8 (2)	1149.1	$(29/2^-) \rightarrow (25/2^-)$	22	1.9(3)
619.1	$(37/2^-) \rightarrow (35/2^-)$	6.0 (9)		1215.1	$9/2^- \rightarrow 9/2^+$	4.1 (6)	2.1(3)
629.0	$5/2^- \rightarrow 1/2^-$	15	1.9 (3)	1400.1	$(45/2^-) \rightarrow (41/2^-)$	5.8 (9)	
633.3	$17/2^+ \rightarrow 13/2^+$	65	1.9 (2)	1419.0	$(47/2^-) \rightarrow (45/2^-)$	5.8 (11)	
634.0	$19/2^+ \rightarrow 15/2^+$	60	1.9 (2)	1486.1	$(35/2^-) \rightarrow (33/2^-)$	4.1 (9)	
657.1		8.0 (11)		1681	$(31/2^+) \rightarrow (29/2^+)$	10	1.5(2)
660.1	$(23/2^+) \rightarrow 19/2^+$	40		1811	$(31/2^+) \rightarrow (29/2^+)$	6.2 (9)	1.5(3)
663.5	$17/2^- \rightarrow 15/2^+$	10	1.3 (2)	2089	$(35/2^-) \rightarrow (33/2^-)$	8.0 (11)	1.6(3)
667.3	$15/2^+ \rightarrow 13/2^+$	35	1.6 (2)	2303	$(33/2^+) \rightarrow (31/2^+)$	8.1 (12)	1.6(2)
668.0	$19/2^+ \rightarrow 17/2^+$	34	1.6 (2)	2382		5.0 (12)	
714.1	$(35/2^+) \rightarrow (33/2^+)$	6.1 (8)		2467	$(35/2^-) \rightarrow (33/2^-)$	5.0 (8)	
720.1	$(41/2^-) \rightarrow (37/2^-)$	6.0 (9)					

[a]The transitions of energies $\leqslant$1500 keV are known to $\sim$0.4 keV; for the higher energies, the uncertainties are $\sim$1 keV.
[b]A blank space is kept for all the transitions for which the spins are not determined.
[c]Except where stated, the uncertainties in relative intensities are less than 10%.
[d]A blank space is kept for all the transitions for which R could not be obtained.

either to the truncation procedure, or to the effective interactions used.

The success of the shell model calculations in ^{94}Tc and in ^{94,95}Mo [5], $^{96-98}$Ru [4], and ^{97,98}Rh [6], points to the desirability of performing similar calculations in ^{95}Tc and ^{96}Tc as well. Figures 8 and 9 show the comparison between the experimental excitation energies and the results of the calculations for ^{95}Tc and ^{96}Tc, respectively.

As seen in Fig. 8, there is a reasonable agreement between the calculated and experimental values using the restricted GL model space up to spin 29/2 $\hbar$ for both the negative- and positive-parity cascades in ^{95}Tc. Notice, however, the discrepancies for the $19/2^+$ and $23/2^+$ levels. This might be indicative of the involvement of orbitals other than those used in this restricted model space. Further, the predicted excitation energy for the $31/2^+$ state is too high in comparison with the measured value. This occurs at the point where the breaking of the $N=50$ core is expected. As in the case of ^{94}Tc, shell-model calculations with the SNE model space have, therefore, been performed for ^{95}Tc. With this large basis space, there is better agreement between experiment and theory for the positive-parity states, and, in particular, the agreement for the $19/2^+$ level is greatly improved. However, the discrepancy for the $23/2^+$ state still persists.

The calculated excitation energies reproduce reasonably well the experimental values for the negative-parity states up to $33/2^-$. Beyond $29/2^+$ and $33/2^-$, the calculations have been performed by incorporating the excitation of a $g_{9/2}$ neutron across the $N=50$ core into the next major oscillator shell [i.e., to the $\nu(d_{5/2}, g_{7/2}, s_{1/2})$ orbitals]. The results of these calculations are indicated in Fig. 8 by an asterisk. Very large gaps occur in the calculations above spin 29/2 $\hbar$ and, clearly, discrepancies still remain between theoretical and experimental excitation energies for the high-spin levels. A similar feature has been observed earlier in the case of ^{96}Ru [4] and ^{94}Mo [5]. Little is known about the effective interactions for such large model spaces (the interactions used in these calculations are a combination of empirical two-body matrix elements and experimental values which were deduced from low-lying energy levels) and it is our hope that the present data will lead to the development of effective interactions more suited to the description of high-spin states in this mass region.

Finally, as shown in Fig. 9, shell model calculations could reproduce the experimental excitation energies only for the 7^+, 9^+, 12^+, and 13^+ levels in ^{96}Tc. Significant discrepancies remain for the energies of the 11^+, 15^+ and 17^+ levels. A similar disagreement had been observed in ^{97}Ru [4].

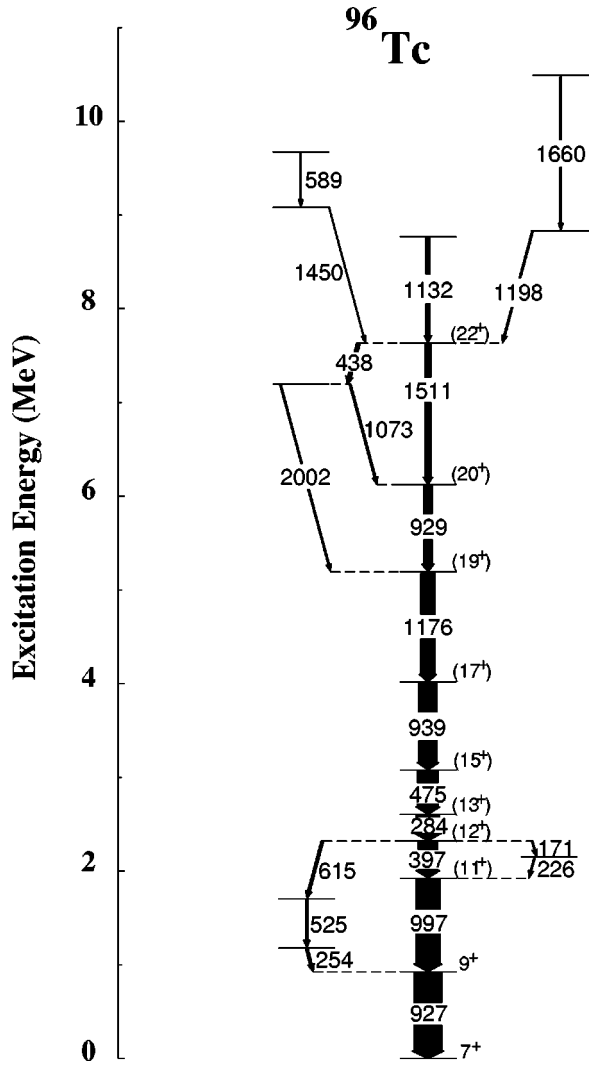

FIG. 5. Level scheme for ^{96}Tc as established from the present study.

TABLE III. Energies, initial and final spins, relative intensities, and ratios R (as defined in the text) for transitions assigned to ^{96}Tc.

E_γ(keV) [a]	$J_i \rightarrow J_f$ [b]	I_γ [c]	R [d]
171.0		5.0 (10)	
226.1		5.0 (9)	
254.0	$(10^+)\rightarrow 9^+$	9.7	1.5 (2)
284.3	$(13^+)\rightarrow(12^+)$	80	1.5 (1)
397.1	$(12^+)\rightarrow(11^+)$	70	1.5 (2)
438.0		13	1.6 (3)
475.3	$(15^+)\rightarrow(13^+)$	71	1.9 (2)
525.0	$(11^+)\rightarrow(10^+)$	9.7	1.5 (2)
589.4		3.3 (7)	
615.2	$(12^+)\rightarrow(11^+)$	9.7	1.6 (2)
927.1	$9^+\rightarrow 7^+$	100	2.0 (1)
929.2	$(20^+)\rightarrow(19^+)$	30	1.9 (2)
939.0	$(17^+)\rightarrow(15^+)$	64	2.1 (2)
997.1	$11^+\rightarrow 9^+$	86	2.0 (2)
1073.2		7.0 (9)	1.5 (3)
1132.1		12	1.5 (2)
1176.3	$(19^+)\rightarrow(17^+)$	49	1.9 (2)
1198.1		8.0 (11)	1.5 (2)
1450.1		4.0 (7)	
1511.2	$(22^+)\rightarrow(20^+)$	21	2.1 (3)
1660		5.3 (8)	
2002		5.4 (7)	1.5 (3)

[a]The transitions of energies $\leqslant$1500 keV are known to $\sim$0.4 keV; for the higher energies the uncertainties are $\sim$1 keV.

[b]A blank space is kept for all the transitions for which the spins are not determined.

[c]Except where stated, the uncertainties in relative intensities are less than 10%.

[d]A blank space is kept for all the transitions for which R could not be obtained.

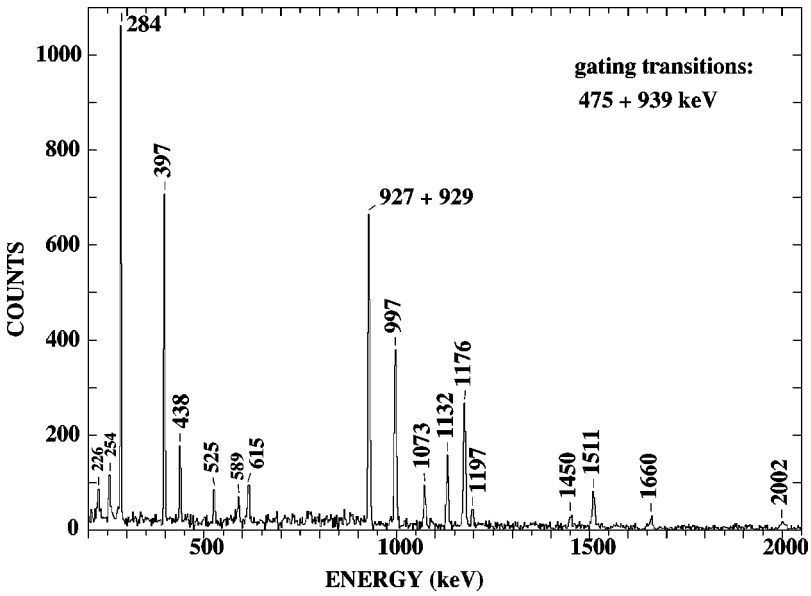

FIG. 6. Representative double-gated coincidence γ spectrum for ^{96}Tc.

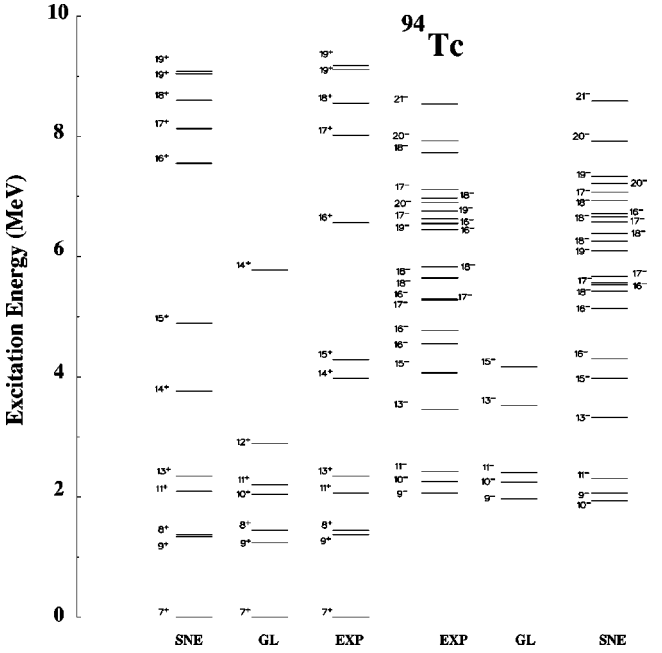

FIG. 7. Comparison of the observed states in ^{94}Tc with the results of spherical shell model calculations, using the small (GL) and large (SNE) configuration spaces, respectively (see text for details).

Again, this may be attributed to contributions from other configurations such as $\nu(g_{7/2},h_{11/2})$ which were not included in the calculations.

V. SUMMARY

The level schemes of ^{94,95,96}Tc ($N=51,52,53$) have been investigated up to high spin ($J\approx 22\hbar$) and excitation energies

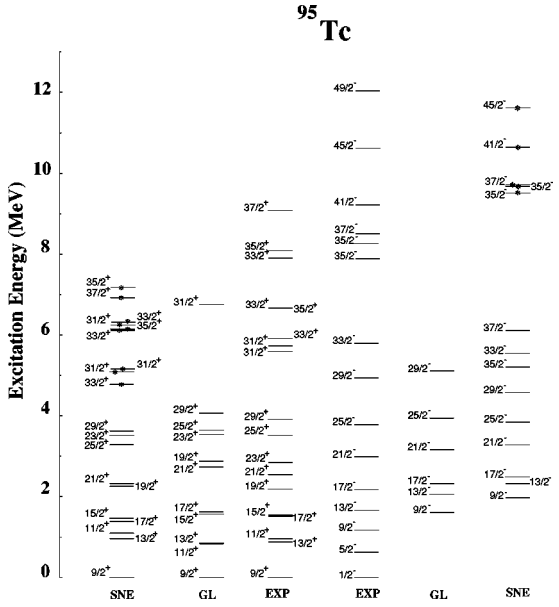

FIG. 8. Comparison of the observed states in ^{95}Tc with spherical shell model calculations, using the small (GL) and large (SNE) configuration spaces, respectively. The levels marked with an asterisk in the calculations include a $g_{9/2}$ neutron excitation across the shell gap (see text for details).

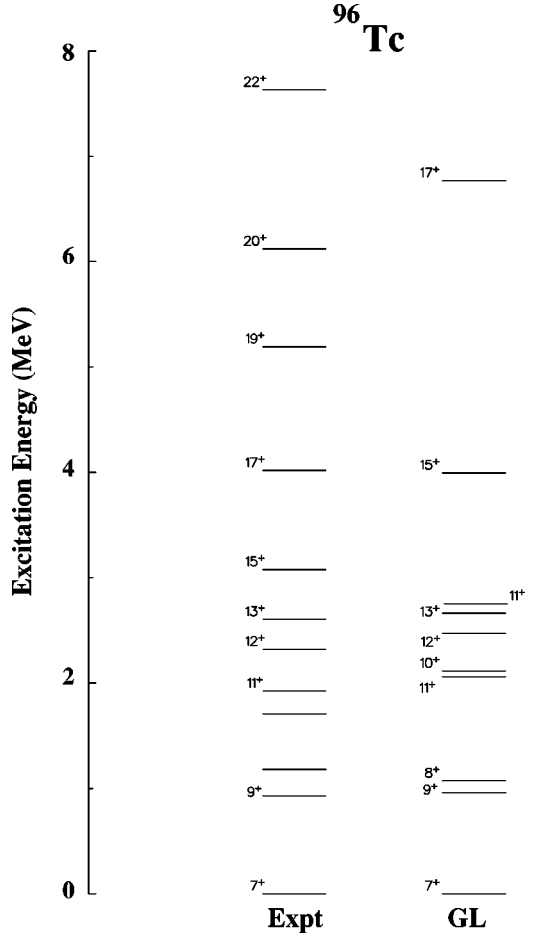

FIG. 9. Comparison of the observed states in ^{96}Tc with spherical shell model calculations using the small (GL) configuration space (see text for details).

($E_x\approx 12$ MeV). The low-lying levels of ^{94}Tc (up to $J^\pi=11^+$ for the positive-parity states, and $J^\pi=15^-$ for the negative-parity sequence) can be described quite satisfactorily as single-particle excitations involving the $[\pi(p_{1/2},g_{9/2});\ \nu(d_{5/2},s_{1/2},g_{7/2},h_{11/2})]$ orbitals. The higher-angular-momentum states are, most likely, dominated by the excitation of a neutron across the $N=50$ closed shell. The level structure of ^{95}Tc can be described rather satisfactorily in the framework of shell-model calculations using a limited configuration space (GL) up to spin $J\approx 29/2\hbar$. For the higher-spin states, the promotion of a $g_{9/2}$ neutron across the $N=50$ shell gap is required to obtain reasonable agreement with the experimental data. Finally, the calculations reproduce the experimental excitation energies for only the 7^+, 9^+, 12^+, and 13^+ levels in ^{96}Tc.

ACKNOWLEDGMENTS

The authors acknowledge the help received from Mr. B. Prause, Dr. G. Smith, and the Gammasphere support staff at LBNL during the experiment. This work was supported in part by the National Science Foundation (Grant Nos. PHY94-02761 and PHY99-01133), the U.S. Department of Energy (Contract Nos. W-31-109-ENG-38 and DE-FG05-87ER40361) and the Polish-American Maria Sklodowska-Curie Joint Fund II (Project No. PAA/DOE-93-153).

[1] S. S. Ghugre, S. Naguleswaran, R. K. Bhowmik, U. Garg, S. B. Patel, W. Reviol, and J. C. Walpe, Phys. Rev. C **51**, 2809 (1995).
[2] S. S. Ghugre and S. K. Datta, Phys. Rev. C **52**, 1881 (1995).
[3] J. Gizon, D. Jerrestam, A. Gizon, M. Jozsa, R. Bark, B. Fogelberg, E. Ideguichi, W. Klamra, T. Lindblad, S. Mitarai, J. Nyberg, M. Piiparinen, and G. Sletten, Z. Phys. A **345**, 335 (1993).
[4] B. Kharraja, S. S. Ghugre, U. Garg, M. P. Carpenter, B. Crowell, R. V. F. Janssens, T. L. Khoo, T. Lauritsen, D. Nisius, W. Mueller, W. Reviol, L. L. Riedinger, and R. Kaczarowski, Phys. Rev. C **57**, 83 (1998).
[5] B. Kharraja, S. S. Ghugre, U. Garg, M. P. Carpenter, B. Crowell, R. V. F. Janssens, T. L. Khoo, T. Lauritsen, D. Nisius, W. Mueller, W. Reviol, L. L. Riedinger, and R. Kaczarowski, Phys. Rev. C **57**, 2903 (1998).
[6] S. S. Ghugre, B. Kharraja, U. Garg, R. V. F. Janssens, M. P. Carpenter, B. Crowell, T. L. Khoo, T. Lauritsen, D. Nisius, W. Reviol, L. L. Riedinger, and R. Kaczarowski, Phys. Rev. C **58**, 3243 (1998).
[7] I. Y. Lee, Nucl. Phys. **A520**, 641c (1990).
[8] D. C. Radford, I. Ahmad, R. Holzmann, R. V. F. Janssens, and T. L. Khoo, Nucl. Instrum. Methods Phys. Res. A **258**, 111 (1987); D. C. Radford, *ibid.* **361**, 297 (1995).
[9] J. A. Kuehner, J. C. Waddington, and D. Prevost, in Procceedings of the International Conference on Nuclear Structure at High Angular Momentum, Ottawa, 1992, edited by J. C. Waddington and D. Ward, Report No. AECL-10613, 1992, p. 413 (unpublished).
[10] T. Shibata, T. Itahashi, and T. Wakatsuki, Nucl. Phys. **A237**, 283 (1975).
[11] D. Hippe, B. Heits, H. W. Schuh, K. O. Zell, H. G. Friederichs, and P. Von Brentano, Z. Phys. A **273**, 349 (1975).
[12] D. G. Sarantites, Phys. Rev. C **12**, 1176 (1975).
[13] G. Winter, F. Dönau, L. Funke, P. Kemnitz, and E. Will, Z. Phys. A **291**, 401 (1977).
[14] K. A. Marshall, J. V. Thompson, W. B. Cook, and M. W. Johns, Can. J. Phys. **56**, 117 (1978).
[15] D. G. Sarantites and A. C. Xenoulis, Phys. Rev. C **10**, 2348 (1974).
[16] H. A. Mach and M. W. Johns, Can. J. Phys. **66**, 62 (1988).
[17] B. A. Brown, A. Etchegoyen, W. D. M. Rae, and N. S. Godwin, MSU-NSCL Report No. 524, 1985 (unpublished).